The co-existence of superconductivity and ferromagnetism in actinide compounds

2003 J. Phys.: Condens. Matter 15 S1945

(http://iopscience.iop.org/0953-8984/15/28/306)

INSTITUTE OF PHYSICS PUBLISHING JOURNAL OF PHYSICS: CONDENSED MATTER

J. Phys.: Condens. Matter **15** (2003) S1945–S1955 PII: S0953-8984(03)62847-X

The co-existence of superconductivity and ferromagnetism in actinide compounds

Andrew Huxley[1], Eric Ressouche[1], Beatrice Grenier[1], Dai Aoki[1], Jacques Flouquet[1] and Christian Pfleiderer[2]

[1] SPSMS-DRFMC, CEA Grenoble 38054, France
[2] Physikalisches Institut, Universität Karlsruhe, Germany

E-mail: huxley@cea.fr

Received 12 November 2002
Published 4 July 2003
Online at stacks.iop.org/JPhysCM/15/S1945

Abstract

Recently superconductivity has been observed in two different 5f-electron ferromagnets, UGe_2 and URhGe, well below their Curie temperatures. While superconductivity could be generic to all clean ferromagnets an alternative possibility is that it occurs in these materials, which were after all carefully selected for study, due to some special features related to the participation of strongly correlated 5f electrons in the ferromagnetism. 5f electrons potentially give rise to strong anisotropies, strong spin–orbit interactions and also a strong energy dependence of the electronic density of states. Here we focus on UGe_2, and review several of the properties of the ferromagnetic state that could be a consequence of such features and discuss whether they promote superconductivity.

(Some figures in this article are in colour only in the electronic version)

1. Introduction

Although superconductivity and ferromagnetism have been established to occur in several materials, UGe_2 represented the first example where the ferromagnetism and superconductivity are clearly not competing orders [1, 2]. Indeed both orders are suppressed simultaneously at a pressure $p_c \approx 16$ kbar.

The superconductivity in UGe_2 is found experimentally only in a limited pressure range (figure 1). In high quality samples traces of superconductivity first appear at pressures of the order $p \approx 10$ kbar where T_x, a temperature at which there is a change in the behaviour of the ferromagnetic state in zero field, becomes small. T_x decreases with pressure and vanishes at a pressure $p_x \approx 12.5$ kbar, close to the pressure at which the superconducting temperature, T_s, is highest. As the pressure is increased there is an abrupt decrease of the ordered moment at p_x and another at p_c in the limit of low field and temperature. Since the magnetization

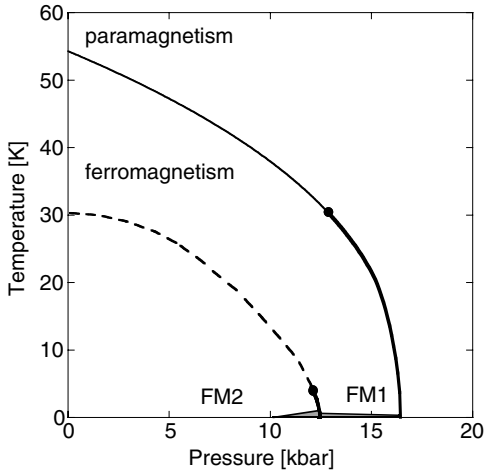

Figure 1. The schematic pressure–temperature phase diagram of UGe_2, described in the text. The thick curves represent first order transitions, thin curves second order transitions and the dashed curve a cross-over. The pressure–temperature region where superconductivity occurs is shaded.

is a first derivative of the free energy this and other observations show that T_x and T_C (the Curie temperature) correspond to first order phase transitions at pressures close to p_x and p_c respectively [3]. The low temperature ferromagnetic state below p_x will be referred to as FM2, the high pressure ferromagnetic state as FM1 and the paramagnetic state above p_c as PM. The position of the critical end point where the first order transition between FM2 and FM1 (i.e. T_x) is replaced by a cross-over, and the position of the tricritical point where the transition to the ferromagnetic state (T_C) changes from first to second order, have not been accurately determined, but are schematically shown as heavy points in figure 1. There are also too few measurements of the pressure dependence of the superconducting transition temperature to establish whether T_s changes discontinuously at p_x as is depicted in the figure.

For pressures above p_x a metamagnetic transition (corresponding to FM1 $\rightarrow$ FM2) occurs for fields parallel to the easy magnetic axis (a-axis). A second metamagnetic transition (corresponding to PM $\rightarrow$ FM1) appears for pressures above p_c. Both metamagnetic transitions are also first order at pressures just above p_x and p_c respectively. If it is assumed that the free energy can be adequately described by a functional of the magnetization density [4], the metamagnetic transitions can be understood to arise as a direct consequence of the two first order transitions at low temperature in zero field. In the limit of low temperature, the field H_x at which the metamagnetic transition associated with p_x occurs increases with pressure, but the transition retains its first order character up to at least 12 T [3], which gives a lower bound for the eventual position of a quantum critical end point (QCEP) for this transition [5]. The field dependence of T_s (or equivalently the upper critical field for superconductivity) in the region of H_x [2, 6] when H_x is not too large is rather interesting (figure 2). The data at low fields in the FM1 phase appear to lie on a different curve (shown schematically) from the points in the FM2 phase as would be expected if there were a discontinuous change of T_s between the two phases. In figure 2 the behaviour at around 1.5 T, which appears to be intermediate between the two limiting behaviours, might indicate that a small fraction of the sample changes to the FM2 state at a lower field than the bulk of the sample. Alternatively, the behaviour at this field might be explained by a very strong dependence of the critical temperature on the proximity to the FM2 $\rightarrow$ FM1 transition. Since the resistive transitions are rather broad (width $\approx$ 100 mK) further experiments are needed to clarify this point.

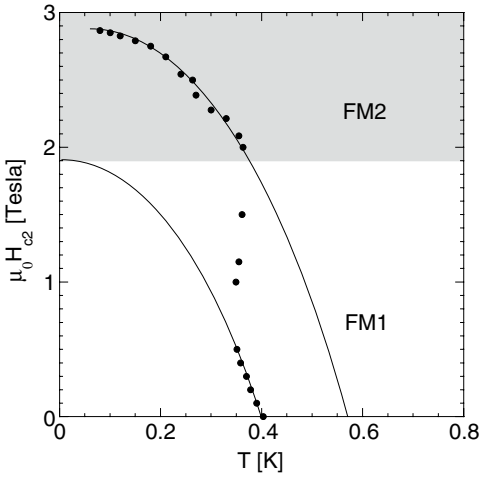

Figure 2. The temperature–field coordinates of the mid-points of the superconducting transitions measured by resistivity are shown at a pressure of 13.5 kbar [2, 6]. The position of the onset of the bulk FM1 → FM2 transition seen in the resistivity in the normal phase at 1 K is also indicated as the lower limit of the shaded region. The lines serve only to guide the eye following the discussion given in the text.

The mechanism responsible for the transition at p_x remains undetermined. It has been suggested that in the FM2 state a spin and charge density wave (CSDW) might be formed due to the nesting of the Fermi surface for one spin polarization [7]. However, extensive neutron diffraction studies [8] have as yet failed to detect any static order due to a CSDW. Other possibilities are that the transition relates to the polarized Fermi surfaces crossing sharp features in the electronic density of states [9] or, as will be developed here, to changes in the localization of some of the f electrons.

The second actinide material in which superconductivity and ferromagnetism were found to co-exist is URhGe where the two orders are present at zero pressure. In both URhGe and UGe_2 there are anomalies in the specific heat at the superconducting transition temperature [10, 11], although for UGe_2 the jump in the specific heat relative to the normal state is only of the order of 10% of the theoretical value for conventional superconductivity. The size of the anomaly is however sufficient to rule out the attribution of the superconductivity to traces of any parasitic phases. The magnitude of the jump in the specific heat also demonstrates that at least some of the f electrons responsible for the enhanced normal state heat capacity are also involved in superconductivity, while neutron studies confirm that the magnetic order also involves uranium f electrons [12].

In the following we begin by reviewing the experimental evidence relating to the itinerant versus local nature of the ferromagnetism. We then present new results that establish that the FM1 phase between p_x and p_c is indeed spatially homogeneous and examine whether there is a change in the degree of delocalization of the f electrons and of the magnetic anisotropy on going from FM2 to FM1. Finally, we examine whether these results can explain the pressure dependence of the superconducting critical temperature.

2. Itinerant ferromagnetism

The initial assertion that the ferromagnetism in UGe_2 is itinerant was based principally on band structure calculations [13, 14] and their qualitative success in accounting for the experimentally

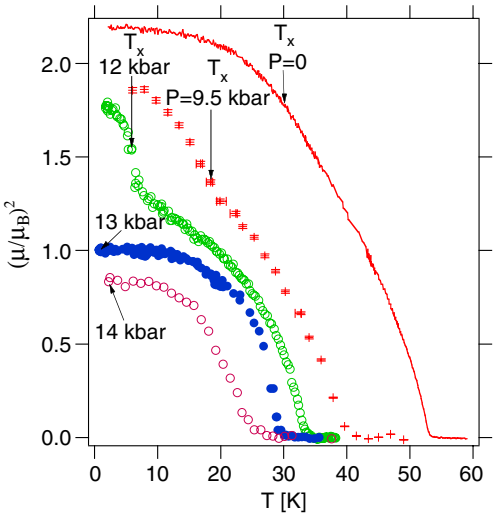

Figure 3. The temperature dependence of the ordered moment squared at different pressures deduced from neutron scattering measurements [2].

observed quantum oscillation frequencies. The agreement is however far from perfect with differences in excess of 20% between the observed and calculated frequencies [15]. The small value of the ordered moment ($\approx$1.5 μ_B for FM2 and $\approx$1 μ_B for FM1), which is considerably smaller than the Curie–Weiss moment (2.8 μ_B at zero pressure) measured above T_C and the observation that the ordered moment continues to increase in an applied field, have also been argued to support the claim that the magnetism is itinerant. Although a small field dependent ordered moment is a characteristic of weak itinerant ferromagnetism, it can also arise under other circumstances. In particular, for the case of localized moments, the mixing of different crystal field levels can give small field sensitive values of the moment [16]. In fact, the temperature dependence of the magnetization in UGe_2 is quite different from that found in weak d-electron itinerant ferromagnets. For these ferromagnets the ordered moment is strongly temperature dependent at low temperatures. For example, the behaviour $(M(T)/M(0))^2 \approx 1 - (T/T^*)^2$ with $T^* \approx T_C$ is found for the archetypal weak d-electron ferromagnet Ni_3Al [17]. This dominates a weaker $T^{3/2}$ dependence due to spin waves that would anyway be absent for UGe_2 due to a strong uniaxial anisotropy. The interpretation of the temperature dependence of the ordered moment in UGe_2 is complicated by the presence of the transition at T_x, particularly at pressures just below p_x. Well away from p_x, however, both at zero pressure and above p_x the magnetization appears to have a different temperature dependence from the above; it obeys the empirical relation $(M(T)/M(0))^2 \approx 1 - (T/T^*)^3$ with $T^* \approx T_C$ at low temperature. This form is somewhat intermediate between that found in the d-metal weak itinerant ferromagnets and the flat form characteristic of a Brillouin function that describes local moment order. This raises the possibility that UGe_2 lies on the border between a local and itinerant behaviour and a change in the degree of localization of some of the f electrons could underlie the transition at p_x. The naive expectation is that pressure increases hybridization and delocalization. In line with this the magnetization in URhGe which has a smaller inter-uranium separation follows more closely a T^2 law. However, for UGe_2 at pressures above p_x the low temperature behaviour of the magnetization appears to be weaker than at pressures well below p_x (figure 3): this suggests that the naive expectation is not fulfilled in this case and instead the higher pressure FM1 phase might have the more localized character.

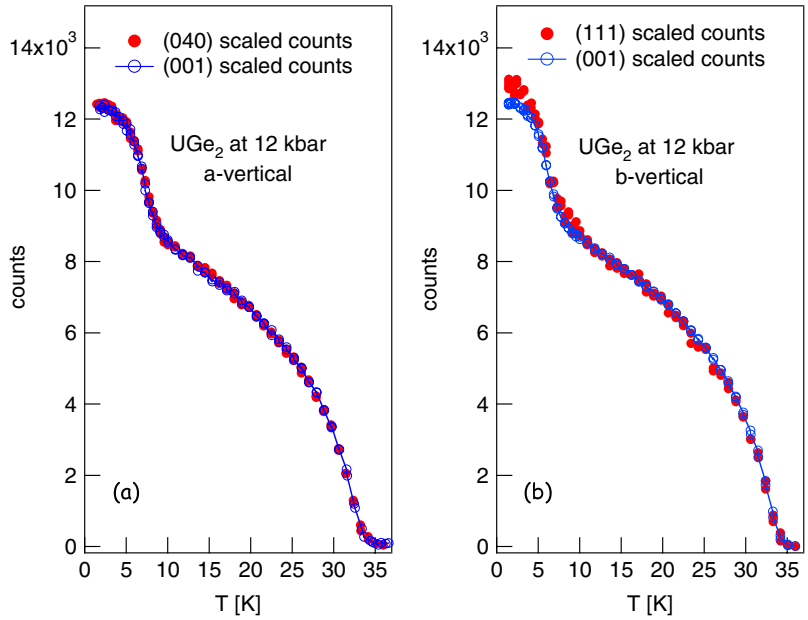

Figure 4. The temperature dependent part of the intensities of different Bragg peaks studied by neutron scattering are compared for two samples of UGe_2 simultaneously pressurized to 12 kbar.

3. Measurements of the magnetic form factor by neutron scattering

A complete polarized neutron diffraction study of UGe_2 at zero pressure has been made by Kernavanois *et al* [12]. In the analysis of such data it is customary to fit the measured moment distribution to single-ion form factors, F_κ, calculated in the dipole approximation. For the case of UGe_2 a fit to either a U^{3+} or U^{4+} form factor describes the data adequately. To be definite we choose the U^{3+} form factor for making comparisons, although the same conclusions are found if the U^{4+} form is chosen. Experimentally, the total moment and the ratio of the orbital to spin moments, $R = -l/s$, are determined from the data (s and l have opposite signs). The magnitude of R is lower than the free ion value due to a partial quenching of the orbital moment, while further changes in the value of R would be expected as a function of pressure if there were changes in the extent of delocalization of the electrons participating in the magnetism. Measurements of the magnetic form factor with polarized neutrons under pressure (at 0 and 14 kbar) by Kuwahara *et al* [18] give $R_{FM1}/R_{FM2} = 1.10 \pm 0.05$. In general, measurements under pressure are difficult since the pressure cell restricts the solid angle over which data can be collected as well as significantly absorbing the incident and diffracted beams.

To complement these measurements we have measured the intensities of several strong magnetic peaks as a function of temperature in zero field at $P = 12$ kbar with the D23-CRG instrument at the ILL (Institute Laue Langevin). A Cu–Be pressure cell of 12 mm external diameter was used with fluorinert as the pressure transmitting medium to reduce the absorption of the neutrons (neutron wavelength 2.37 Å). Two samples oriented respectively with (100) and (010) axes perpendicular to the diffraction plane were measured in the same experiment. At this pressure the transition at T_x is strongest and is easily visible in the data (figures 4 and 5). The measurements for both samples were made successively without warming the pressure cell to above 60 K. In figure 4 the temperature dependence of the diffracted intensities of different

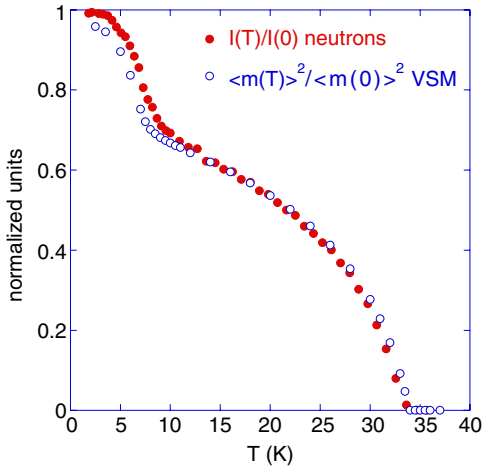

Figure 5. The normalized temperature dependence of the intensity of the (001) Bragg peak in UGe_2 is compared to the magnetic moment squared measured in a VSM at an almost equivalent pressure of 12 kbar.

peaks are compared. The peak intensities were measured as a function of temperature without moving the spectrometer or the detector with the detector positioned at the position of maximum intensity. This gives an improved sensitivity compared to measuring a complete rocking curve at each temperature to give the integrated intensity since it avoids small repositioning errors that otherwise give rise to an overall lower resolution of about 1%. To control the validity of this method the peak profiles were measured at the lowest and highest temperatures to confirm that the form of the profiles did not change.

The measured temperature dependences of the (001) and (040) peaks are seen to be identical (figure 4(a)). These two peaks have almost identical Bragg angles, but are sensitive to moments in different directions (perpendicular to q in each case). The accurate scaling of their intensities therefore implies that it is unlikely that there is any change in the orientation of the moments (which therefore remain oriented along $\boldsymbol{a}$) as the transition at T_x is crossed.

The scaling for the (001) and (111) peaks is however not quite perfect (figure 4(b)). There is a relative increase in the strength of the (111) peak by $4 \pm 1\%$ below T_x relative to the (001) peak. These peaks have different Bragg angles; $\sin(\theta)/\lambda = 0.179$ for the (111) peak, while $\sin(\theta)/\lambda = 0.123$ for the (001) peak (θ is the Bragg angle). The relative increase in the strength of the (111) peak below T_x can be related to a change in R and gives $R_{FM1}/R_{FM2} = 1.15 \pm 0.04$. The ratio of the orbital to the spin moment thus appears to be slightly larger in the high pressure FM1 phase, in agreement with the observations of Kuwahara *et al* [18]. This is contrary to the naive expectation that $-l/s$ would decrease with pressure due to a greater delocalization of the f orbitals, but in line with the flatter temperature dependence of the magnetization described earlier. In reality the value of $-l/s$ is made up from contributions from different bands and also includes interband terms. Band structure calculations suggest that there are two main majority spin sheets, whereas experimentally at p_x only one of these sheets appears to be significantly modified [19]. A more complete analysis would require identifying the contribution to the overall value of l/s from these different sources.

Finally, in figure 5 we compare the variation of the moment squared deduced from the magnetization with the neutron data for the (001) peak. The two curves have a similar form, but the T_x values are slightly different due to a small difference in the pressure between the two

measurements. The neutron scattering measures $\langle {F_\kappa}^2 M^2 \rangle$ averaged over the sample, whereas the direct measurement of the magnetization measures $\langle M \rangle$. We have already shown that ${F_\kappa}^2$ changes by only a few per cent on going from the FM1 phase to FM2. If the ferromagnetism above p_x were inhomogeneous however $\langle M \rangle^2 \neq \langle M^2 \rangle$. In the limit that the sample in FM1 was divided into magnetic and non-magnetic regions this would lead to a large discrepancy between the two curves, much larger than observed experimentally. For example, suppose that FM1 comprised two-thirds of the sample in the FM2 state (1.5 μ_B) while the remaining one-third was paramagnetic. Then $\langle M \rangle^2 = 1\ {\mu_B}^2$ while $\langle M^2 \rangle = 1.5\ {\mu_B}^2$. Thus if the two curves were scaled to give agreement in the FM2 phase a discrepancy of 50% would be apparent in the FM1 phase, which is clearly not the case. We can thus rule out the possibility that a significant part of the sample is non-magnetic above p_x or that there is a significant contribution from s, p or d electrons to the ordered moment in the FM1 state; such electrons would have a form factor that is sharply peaked at $q = 0$ and not contribute to the neutron measurement.

4. Anisotropy

In the previous section we found no evidence for a change in the direction of the ordered moment with pressure in UGe_2. This is supported by the observation that fields applied parallel to the easy axis have a large effect on the phase diagram of figure 1, while fields in the perpendicular directions have little effect [2]. In this and the next section we will consider the differential susceptibility $\mathrm{d}M/\mathrm{d}H$, since it is this that gives a measure of the spectrum of the magnetic excitations. The inverse susceptibilities of UGe_2 and URhGe along different crystal axes above T_C at zero pressure are shown in figure 6. The susceptibility for URhGe near T_C is clearly less strongly uniaxial than for UGe_2. It is important to note that the space groups of the two materials are different (the space groups of URhGe and UGe_2 are respectively $Pnma$ and $Cmmm$). As a consequence the magnetic moments in URhGe can simultaneously have an anti-ferromagnetic ordered component directed along the $\boldsymbol{a}$-axis in addition to a ferromagnetic component parallel to the $\boldsymbol{c}$-axis without lowering the symmetry further. The susceptibility for $H \parallel b$ in URhGe indeed looks like that of a material approaching an antiferromagnetic transition. Neutron scattering measurements nevertheless show that below T_C URhGe is a simple collinear ferromagnet [11, 20] with moments parallel to the $\boldsymbol{c}$-axis despite some incorrect reports in the literature to the contrary [21]. For UGe_2 the magnetic space group representations contain moments aligned to a single axis only. In the next section we will focus on the differential susceptibility at low temperature in the ferromagnetic state of UGe_2. At low pressures we find that $\mathrm{d}M/\mathrm{d}H$ is much more isotropic than close to p_c. The similarity of the crystal structure of UGe_2 with that of URhGe suggests that the anisotropy between the 'easy' $\boldsymbol{a}$-axis and $\boldsymbol{c}$-axis directions of UGe_2 could be of particular interest. An unusual hysteresis in measurements of the superconducting critical field for pressures very close to p_c for fields parallel to the $\boldsymbol{c}$-axis [6] also single out the $\boldsymbol{c}$-axis for investigation. Therefore we have limited our study to the pressure dependence of M for fields parallel to the $\boldsymbol{a}$-axis and $\boldsymbol{c}$-axis to date.

5. Magnetic measurements in a magnetometer under pressure

In figure 7 the longitudinal magnetization of UGe_2 determined at 2.3 K in a vibrating sample magnetometer (VSM) for fields parallel to the $\boldsymbol{c}$-axis (a hard magnetic axis) at several pressures is shown. Since the sample in the pressure cell is never perfectly aligned to the field there is always a small component of the applied field parallel to the easy magnetic

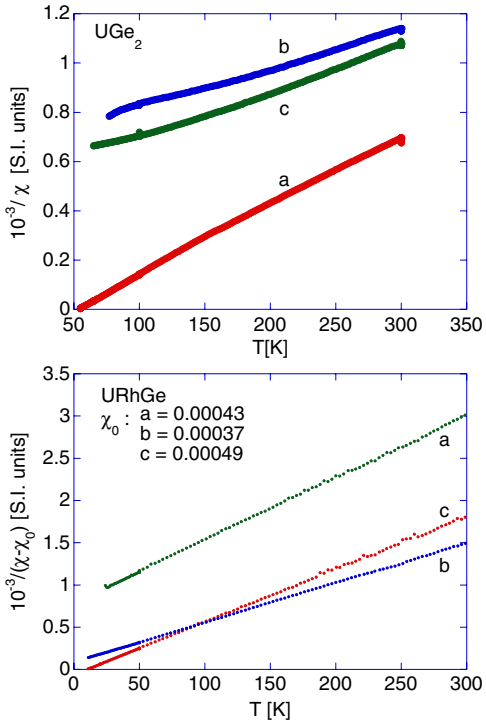

Figure 6. The two panels show the inverse susceptibility for UGe_2 and URhGe in their paramagnetic states at zero pressure along different crystal directions. For the latter an almost isotropic term has been subtracted from χ; when plotted in this way Curie–Weiss behaviours are found along all three axes.

axis, $H\sin(\theta)$, where θ is the misorientation of the $\boldsymbol{a}$-axis from the plane perpendicular to the axis of the magnetometer. The total magnetization parallel to the applied field is then $M_z = M_c\cos(\theta) + M_a\sin(\theta)$. For $H\sin(\theta) < H_{coer}$ where H_{coer} is the coercive field, the magnetization M_a dominates the response. However, for $H\sin(\theta) > H_{coer}$ the sample becomes monodomain along the easy axis, and the subsequent field dependence of the measured magnetization, M_z, is due principally to changes of M_c. The slope of the curves in figure 7 at low fields can therefore be attributed to the transverse magnetization and a small misalignment of the sample, while the slope above the knee in the curves at high fields gives a measure of $(\mathrm{d}M/\mathrm{d}H)_c$. The exact field at which the knee occurs depends on the inclination of the sample. The high field susceptibility deduced from a linear fit to the slope above the knee (with the transverse magnetic domain structure saturated) is shown as a function of pressure in figure 9. The magnetization measured for fields parallel to the $\boldsymbol{a}$-axis is shown in figure 8 [3]. The differential susceptibility $(\mathrm{d}M/\mathrm{d}H)_a$ is clearly seen to be different in the different magnetic phases FM1 and FM2, but must be distinguished from the tails of the rapid changes at the metamagnetic transitions. To be definite we take $(\mathrm{d}M/\mathrm{d}H)_a$ in the FM1 and PM phases to be equal to its minimum value over the range of fields where each phase exists at a given pressure. The value for the FM2 phase is taken to be the average value over the range 5–10 T. The values of $(\mathrm{d}M/\mathrm{d}H)_a$ deduced are weakly sensitive to the details of these definitions, but the clear jump in $(\mathrm{d}M/\mathrm{d}H)_a$ between the FM2 and FM1 phases is clearly independent of such details.

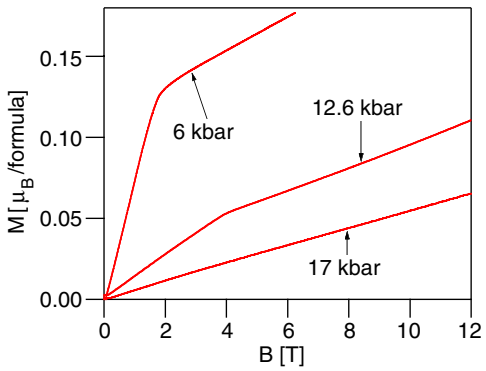

Figure 7. The magnetization of UGe_2 at 2.3 K measured in a VSM relative to that of the empty pressure cell is shown for fields almost parallel to the crystal ***c*** axis.

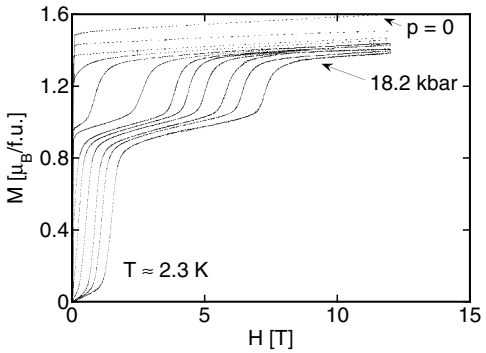

Figure 8. The magnetization of UGe_2 at 2.3 K measured in a VSM relative to that of the empty pressure cell is shown for fields parallel to the crystal ***a***-axis [3]. The pressures are 0, 6.5, 9, 11.1, 12.8, 13.8, 15.3, 15.5, 16, 16.7, 17.3 and 18.2 kbar.

The main conclusion is that the differential susceptibility (figure 9) is strongly anisotropic in the FM1 and PM phases but only weakly anisotropic in the low pressure FM2 phase. Since $\mathrm{d}M/\mathrm{d}H$ gives a measure of the spectral weight of ferromagnetic excitations for each moment direction, we conclude that at low pressure there are as many modes perpendicular to the ordered moment as parallel to it. The latter favour magnetically mediated triplet superconductivity while the former are pair breaking. The increase in anisotropy at high pressure, in the FM1 phase, is therefore a favourable factor for the formation of superconductivity at these pressures. Superconductivity however does not occur in the PM phase where a large anisotropy is also present. The absence of superconductivity in the PM phase therefore requires a different explanation, such as the presence of a competing singlet scattering mechanism that is suppressed by the splitting of the oppositely spin polarized bands in the ferromagnetic state.

The relative increase of $(\mathrm{d}M/\mathrm{d}H)_a$ on going from FM2 to FM1 is approximately twice as large as the relative increase in the low temperature specific heat [10]. For isotropic materials and purely itinerant magnetism the Pauli susceptibility and specific heat coefficient would be proportional. The increase in the differential susceptibility seen in UGe_2 however is much larger than that of the specific heat indicating that such a simplified analysis does not hold in the present case.

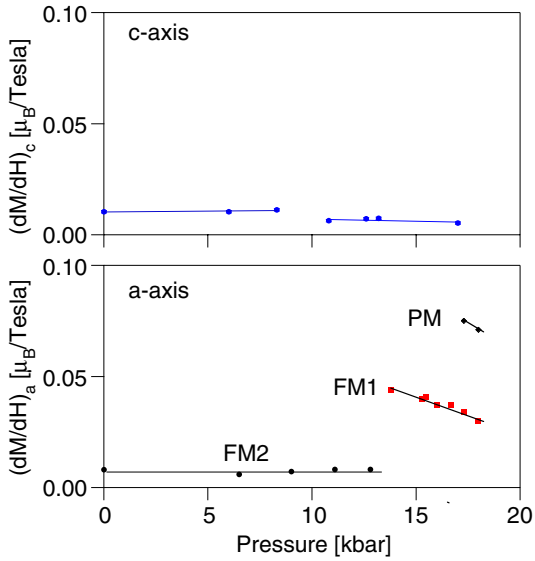

Figure 9. The differential susceptibility (defined in the text) is shown parallel to the c-axis in the upper panel and parallel to the a-axis in the lower panel, where the values measured in the different magnetic phases (FM1, FM2 and PM = paramagnetic) are distinguished.

6. Conclusions

We have described evidence that establishes that the ferromagnetic FM1 state is homogeneous. It is distinguished from the low pressure FM2 state by a large decrease in the value of the ordered moment of 30% and by a large increase in the electronic specific heat (300%). We have shown here that this is accompanied by a very modest increase in the ratio of the orbital to spin moment but a large increase in the magnetic anisotropy ($>600\%$). These changes and the flatter temperature dependence of the magnetization in the FM1 state would suggest that contrary to expectations the FM1 state appears to have the more localized magnetic character. One consequence for superconductivity is that the differential susceptibility is strongly uniaxial at low temperature only at high pressure. A strong anisotropy with a large value of $\mathrm{d}M/\mathrm{d}H$ parallel to the ordered magnetic moment and small values of $\mathrm{d}M/\mathrm{d}H$ for directions perpendicular to the ordered moment is a favourable factor for triplet superconductivity since pair forming excitations then outweigh pair-breaking fluctuations.

It is plausible that the change in anisotropy is directly related to a shift to a more localized character of the magnetization in the FM1 phase. This suggests that an intermediate degree of electron localization could be an important factor in understanding the mechanism for superconductivity. To date, calculations have not considered this explicitly, but either have been based on a local moment starting point [22, 23] or have considered the superconductivity to appear from a completely itinerant ferromagnetic state.

References

[1] Saxena S *et al* 2000 *Nature* **406** 587
[2] Huxley A D *et al* 2001 *Phys. Rev.* B **63** 144519
[3] Pfleiderer C and Huxley A 2002 *Phys. Rev. Lett.* **89** 147005
[4] Yamada K 1993 *Phys. Rev.* B **47** 11211

[5] Grigera S A *et al* 2001 *Science* **294** 329
[6] Sheikin I *et al* 2001 *Phys. Rev.* B **64** 220504(R)
[7] Watanabe S and Miyake K 2002 *Physica* B **312/313** 115
Watanabe S and Miyake K 2002 *J. Phys. Chem. Solids* **63** 1465
[8] Flouquet J *et al* 2001 *J. Phys. Soc. Japan Suppl.* A **70** 14
[9] Sandeman K G, Lonzarich G G and Schofield A J 2003 *Phys. Rev. Lett.* **90** 167005
[10] Tateiwa N *et al* 2000 *J. Phys.: Condens. Matter* **13** L17
[11] Aoki D *et al* 2001 *Nature* **413** 613
[12] Kernavanois N *et al* 2001 *Phys. Rev.* B **64** 174509
[13] Shick A B and Pickett W E 2001 *Phys. Rev. Lett.* **86** 300
[14] Yamagami H unpublished
[15] Settai R *et al* 2002 *J. Phys.: Condens. Matter* **14** L29–36
[16] Yang Y L and Cooper B R 1969 *Phys. Rev.* B **185** 696
[17] Lonzarich G G *et al* 1987 *J. Magn. Magn. Mater.* **54** 612
[18] Kuwahara K *et al* 2002 *Physica* B **312/313** 106
[19] Terashima T *et al* 2001 *Phys. Rev. Lett.* **87** 166401
[20] Ressouche E 2002 unpublished
[21] Prokes K 2002 private communication
Prokes K *et al* 2002 *Physica* B **311** 220
[22] Suhl H 2001 *Phys. Rev. Lett.* **87** 167007
[23] Abrikosov A A 2002 *J. Phys.: Condens. Matter* **13** L943